Enhancement of polylactic acid films properties by incorporation of starch nanocrystals

Paola Chaves Martins [1] | Juliana Machado Latorres [1] | Ana Vera Machado [2] | Vilásia Guimarães Martins [1]

[1] School of Chemistry and Food Engineering, Laboratory of Food Technology, Federal University of Rio Grande (FURG), Rio Grande, Brazil
[2] Institute for Polymers and Composites, Minho University, Braga, Portugal

Abstract

Polylactic acid (PLA) is a biodegradable polymer used in films production; however, it has some limitations. Thus, strategies can be used to improve the characteristics of these materials such as the incorporation of starch nanocrystals (SNCs). Therefore, the aim of this study was to add potato and rice SNCs in PLA matrix in the melt to obtain PLA films with structural reinforcement to improve its properties. The SNCs were produced by acid hydrolysis and incorporated to the matrix in 0.5 and 1wt% amounts. The films were then produced by bioriented tubular extrusion and characterized with several techniques. Films containing 1wt% of potato SNCs showed an increase in tensile strength, elongation, and glass transition temperature, but a reduction in water vapor permeability. Therefore, the use of potato SNCs as a structural reinforcement for PLA films improved the properties of the films making them suitable candidates for several other applications.

KEYWORDS

biodegradable, biomaterials, extrusion, functionalization of polymers, thermoplastics

1 | INTRODUCTION

Polymers of synthetic origin are widely used industrially to produce different types of packaging. The packaging has some main functions such as, contain, protect, and communicate. Conventional polymers provide to the packaging excellent properties, however, its use on a large scale causes environmental impact, since most of it is not recycled contributing to an increase in waste. [1] Several sustainable and environmentally friendly materials have been studied to replace polymers derived from petroleum-based sources. [2]

Polylactic acid (PLA) is thermoplastic aliphatic polyester that has been produced from renewable resources by fermentation processes. It has been classified as a "green" polymer due to its sustainability and biodegradability. [3] PLA has been widely applied in the production of films for food packaging [4] and medical devices. [5] Packages produced from PLA have advantages such as high rigidity, however, they have low thermal resistance and deficient barrier properties when compared with conventional polymers. [6] Some strategies have been studied and applied to improve the properties of PLA films, such as the use of nanometric structural reinforcements. [7]

Starch is a polysaccharide widely found in different botanical sources such as corn, rice, potatoes, cassava and others. [8] Structurally, starch is composed of amylose and amylopectin molecules that are radially arranged in the starch granule forming alternating crystalline and non-crystalline regions. [9] The crystalline regions that compose the starch structure can be isolated and originate a highly reactive nanomaterial, such as nanocrystals. Nanocrystals can be obtained through acid [10] and enzymatic [11] hydrolysis processes or the combination of chemical and physical methods. [12] When the acid hydrolysis process is used in starch granules, the breakdown of glycosidic bonds occurs in the amorphous part of the molecules and subsequently in the crystalline part, promoting the release of highly crystalline residues on a nanometric scale producing the starch nanocrystals (SNCs). [13] As the size of a particle decreases to the nanoscale, important changes occur in the surface area making these molecules reactive due to the abundance of hydroxyl groups available for other bonds. [14] The incorporation of SNC in polymeric matrices forms nanocomposite films that have specific properties, such as a strong structural reinforcement effect and a positive impact on barrier properties. [15]

Different compounds have been reported in the literature as structural reinforcement agents for PLA films, such as cellulose nanofibrillated, [16] cellulose nanocrystals, [17] quinoa starch nanocrystals, [18] waxy maize starch nanocrystals [7] and others. However, information on the behavior and characterization of starch nanocrystals obtained from a hydrolytic process in the matrix of PLA films inserted by an extrusion process is less explored. Based on the above, this study aims to investigate the incorporation of potato SNCs and rice SNCs obtained from the hydrolytic process of starch on the properties of PLA film obtained by tubular extrusion.

2 | MATERIAL AND METHODS

1 | Material

Polylactic acid (PLA) used in this study was the PLA F15C obtained from the company Inzea Biopolymers. PLA F15C is composed of 52% PLA and 48% starch and has a melt temperature of 130°C. Rice and potato starches were supplied by Horizonte (Paraná, Brazil). The sulfuric acid used to obtain the nanocrystals was produced by Synth with a purity of 98%.

2 | Starch nanocrystals production

The nanocrystals were prepared as described by Zhou et al.. [19] The potato and rice starches were fractionated separately in portions of 25 g and homogenized with 250 ml of H_2SO_4 3.16M. The suspensions were placed in an orbital shaker at 100rpm, 40°C for 7 days. Afterwards, the suspensions were washed with distilled water and centrifuged at 1000 × g for 10 min successive times until neutral pH . The precipitates were lyophilized to obtain the nanocrystals.

3 | Characterization of SNCs

1 | X-ray diffraction

X-ray diffractograms were analyzed using X-ray diffractometer (Bruker, D8 Advance, US) with a voltage of 40 kV , a current of 40 mA , using copper tube and 1.54Å. The samples were scanned within the range of 2θ in the region of 3 to 40°.

2 | Scanning electron microscopy

SNCs granules and native starches were evaluated using a scanning electron microscope (SEM) (JEOL, JSM6610 LV , US). The samples were covered with a gold layer to increase the conductivity. The voltage used was 10 kV and the magnification used was 2000 ×.

3 | Thermogravimetric analysis

The thermal behavior of the SNCs was determined using TGA (TA instruments TGAQ500, US). The amount of sample used was between 2 and 5 mg and the scanning temperature applied was from 30 to 600°C. The nitrogen rate applied was 40ml/min and the temperature variation used was 10°C/min.

4 | Production of PLA/SNCs nanocomposite pellets

PLA pellets incorporated with SNCs were prepared in a twin-screw extruder (Leistritz LSM 96/25 D, Germany), using a screw speed of 125 rpm , a feed flow of 3 kg/h and a constant temperature of 120°C along the barrel. The nanocrystals of rice starch (RSNCs) and potato starch (PSNCs) were incorporated into the PLA separately at concentrations of 0.5 and 1.0wt%. PLA was first fed at the hopper at the beginning of the barrel, then the SNCs were fed through a second hopper. Two different amounts (0.5 and 1 wt% of RSNCs PSNCs) were used, respectively.

5 | PLA/SNCs films production

The films with the composition described in Table 1 were produced in a bioriented single-screw tubular extruder (Extrusora O25X25D, Portugal) with a feed rate of 2.7 kg/h and a screw speed of 50 rpm . The temperatures along the extrusion barrel were zone A 120°C, zone B

TABLE 1 Composition of the several films produced and the corresponding codes

Polymer	Additive	Code
Polylact acid (PLA)	-	PLA
	0.5% rice starch nanocrystals	PLA/RSNCs 0.5wt%
	1% rice starch nanocrystals	PLA/RSNCs 1wt%
	0.5% potato starch nanocrystals	PLA/PSNCs 0.5wt%
	1% potato starch nanocrystals	PLA/PSNCs 1wt%

140°C, and zone C150°C at the die. The used rolls speed was 3.6 m/s, the standard film width was 14 cm , the pull rate was through the opening of 1.8 cm , and the average film thickness was 50μ m.

6 | Characterization of PLA films

1 | Color and opacity

Color and opacity were validated using a colorimeter (Minolta, CR-400, Japan), and the CIELab color space was used. The color of the films was expressed as the total difference in color (ΔE^*) by Equation 1 obtained using illuminant D65. The parameters analyzed in this color system are L* (lightness/brightness), a* (red-ness/greenness), and b* (yellowness/blueness). Opacity (0_P) was calculated according to Sobral et al. [20] using Equation 2, where Y_b represents the black standard and Y_w is the white standard of each evaluated film.

$$\Delta E* = \sqrt{(L* - L*_s)^2 + (a* - a*_s)^2 + (b* - b*_s)2} \quad (1)$$

$$OP(\%) = (Yb/Yw) \times 100 \quad (2)$$

2 | Contact angle measurements

The contact angle of the films was evaluated using a microscope in static mode (Contact Angle System OCA 20, Germany). The contact angle was measured using water as a solvent in the amount of 3μl and with a drop generation speed of 2μl/s. The contact angle was measured in triplicate of each treatment and through the media of five drops. As the drop was deposited on the film surface the image was recorded by the SCA 20 software to calculate the angle formed.

3 | Mechanical properties

The films were characterized through tensile strength (TS), elongation at break (EB), and elastic modulus (EM) using an Extensometer (ZwickRoell Z005, Germany) according to the ASTM Standard Method D882-02. [21] The films were cut into 10 strips of 10 × 1.5 cm in transversal and longitudinal orientation. The test speed was 200 mm/s, post-test speed of 500 mm/s and separation distance of the claws 50 mm .

Dynamic mechanical variation (DMA) was evaluated using a DMA (Tryton T101423D TTDMA, UK). Loss modulus (E''), storage modulus (E'), and tan delta (E''/E') were determined. The films of 30×5 mm was analyzed in a temperature range from 30 to 100°C, using a heating rate of 5°C/min, a dynamic force of 1 N and the frequency of 1 Hz .

4 | Water vapor permeability

Water vapor permeability (WVP) was evaluated according to ASTM Standard Method E96-00. [22] The mass variations of the permeation cell were measured every 24 h for 7 days. The WVP was calculated using Equation 3.

$$\text{WVP (g.mm/m2.day.kPa)} = \text{W.L/A.t. } \Delta P \quad (3)$$

where W is the weight gain of the permeation cell (g), L is the film thickness (mm), A is the exposed area of the film (m^2), t is the time of weight gain (day), and ΔP is the vapor pressure difference across the film (kPa).

5 | Oxygen permeability

The OP of the films was evaluated in a gas diffusion permeabilimeter (Porous Materials DP-100A, US). The analysis was performed in duplicate using circles of 5 cm in diameter of each film. The film was placed in a vacuum gas permeation chamber with an exposed area for oxygen permeation. The equipment measures the amount of oxygen ($\text{ml.mm/MPa/min/cm}^2$) that passed through the length of the film in the period of 3 h .

6 | Thermal properties

The thermal behavior of PLA and PLA/SNCs nanocomposite films was determined using TGA (TA instruments TGAQ500, US), as described for the thermal characterization of the SNCs.

7 | X-ray diffraction

The crystallinity of the films was evaluated using X-ray diffractograms obtained from X-ray diffractometer (Bruker, D8 Advance, USA). The scan was performed in 2θ in the region of 3 to 40°. The voltage used was 40 kV , the current was 40 mA , using copper tube and 1,54Å. The RC (%) of the films was calculated by the Equation 4, Ac is the crystalline area, and Aa is the amorphous area on the X-ray diffractograms.

$$\text{RC} = (\text{Ac}/(\text{Ac} + \text{Aa})) \times 100 \quad (4)$$

8 | Scanning electron microscopy

The microstructure of the films was evaluated using a scanning electron microscope (NOVA 200 NanoSEM, US) with electron acceleration voltage between 5 and 10 kV . The films were cut transversely using liquid nitrogen to break the structure and afterwards were covered with a gold layer to amplify the conductivity of the materials. The approximation applied in the analysis was 3000 ×.

7 | Statistical analysis

The analyzes were carried out in triplicate and from that the means and standard deviation were calculated. Analysis of variance (ANOVA) was used followed by Tukey's test for the determination of significant differences with 95% confidence interval.

3 | RESULTS AND DISCUSSION

Characterization of SNCs

The nanocrystals used as structural reinforcement of the PLA films developed in this study were previously elaborated and extensively characterized according to the study of Martins, Latorres, and Martins. [23] More details about structural and thermal characterizations are presented in Figure 1-3. The micrographs of native starches and SNCs are shown in Figure 1a-d. Native rice starch and native potato starch differ in their morphology due to their different botanical characteristics. Rice is a cereal that has smaller granules, an irregular structure and straighter corners. The SNCs (Figure 2c) obtained show that the granule structure was affected by the acid process, since the morphology of the granules was modified and it perceived the agglomeration of the granules after the process. The potato is classified as a tuber and has larger starch granules, with defined structure and rounded corners. The SNCs (Figure 2d) produced from potato starch was strongly attacked by the hydrolysis process. The granules were degraded and formed crystals with straight and fractured boundaries. Similar behavior was described by Zhou et al., [19] the author also suggested that the tendency of SNCs agglomeration occurs due to the presence of a large number of $OH-$ groups exposed during the hydrolysis process and that are capable of being linked by hydrogen bonds.

XRD has been widely used to evaluate changes in crystalline structures due to physical or chemical modifications. [19] Figure 2a shows the diffractograms and relative crystallinity for native starch and SNCs. The hydrolysis applied to the production of the SNCs for both starches increased the relative crystallinity more than 3 times when compared with the crystallinity of native starch. It is possible to observe that the peaks of the SNCs were less defined and with greater amplitudes, contributing to this increase in the percentage of crystallinity. The hydrolysis process applied to obtain the nanocrystals acts by breaking bonds in the amorphous part of the starch, maintaining the crystalline part, consequently increasing the degree of crystallinity. [24] The same behavior of increased crystallinity with the application of hydrolysis has been reported in other studies. [11,25] Second [26] the high crystallinity that the SNCs present can act as a structural reinforcement when added in film matrices. The high crystallinity of this material can contribute to increase the crystallinity of the films, improving the general properties of the packaging.

The thermogram of the rice and potato starch SNCs (Figure 2b) presents two stages, the first with temperatures around $150°C$ where the starches exhibited approximately a weight loss of 10% and the second stage at $330°C$ where the starches present around 60% weight loss. According to Dufresne, [13] the presence of two peaks is common in SNCs and this behavior is attributed to the heterogeneity of the crystallinity of the material. The dense crystalline part is only degraded at higher temperatures presented in the second weight loss zone (around $300°C$). The behavior of the thermogram in Figure 2b was the same for both types of SNCs, however, the differences noticed in the temperatures are related to the

botanical characteristics of the materials that are obtained from different sources of starch. According to Lecorre et al., [27] the differences in amylose/amylopectin content, structural organization, crystallinity and other composition materials directly interfere in the thermal properties of the materials. In general, the temperature of greatest weight loss of the native starches is around 300°C, however, when SNCs are produced applying the hydrolysis process with sulfuric acid, the sulfate groups of the acid may be present on the surface of the SNCs and catalyze the depolymerization increasing the

FIGURE 1 Micrographs (a) native rice starch, (b) native potato starch, (c) rice SNCs, and (d) potato SNCs

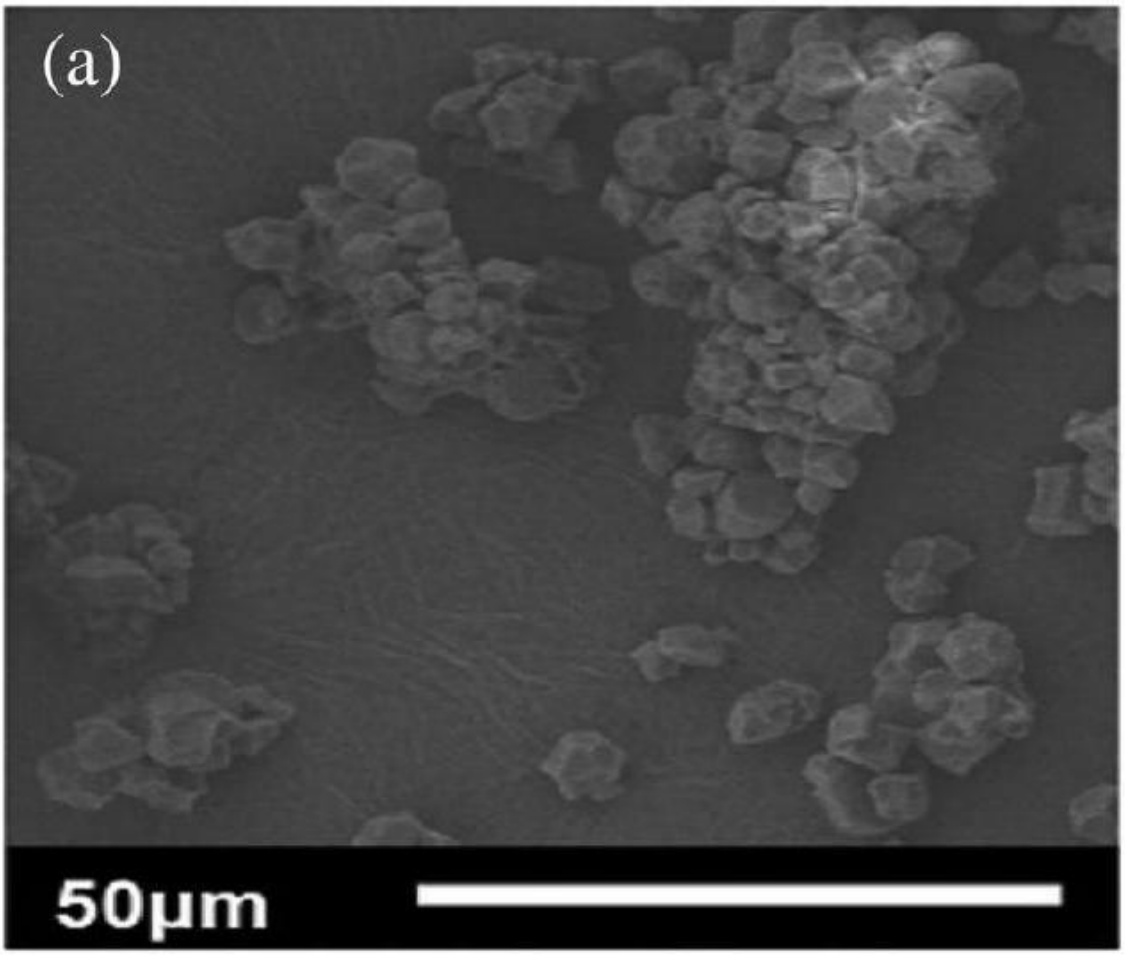
(a)
50μm

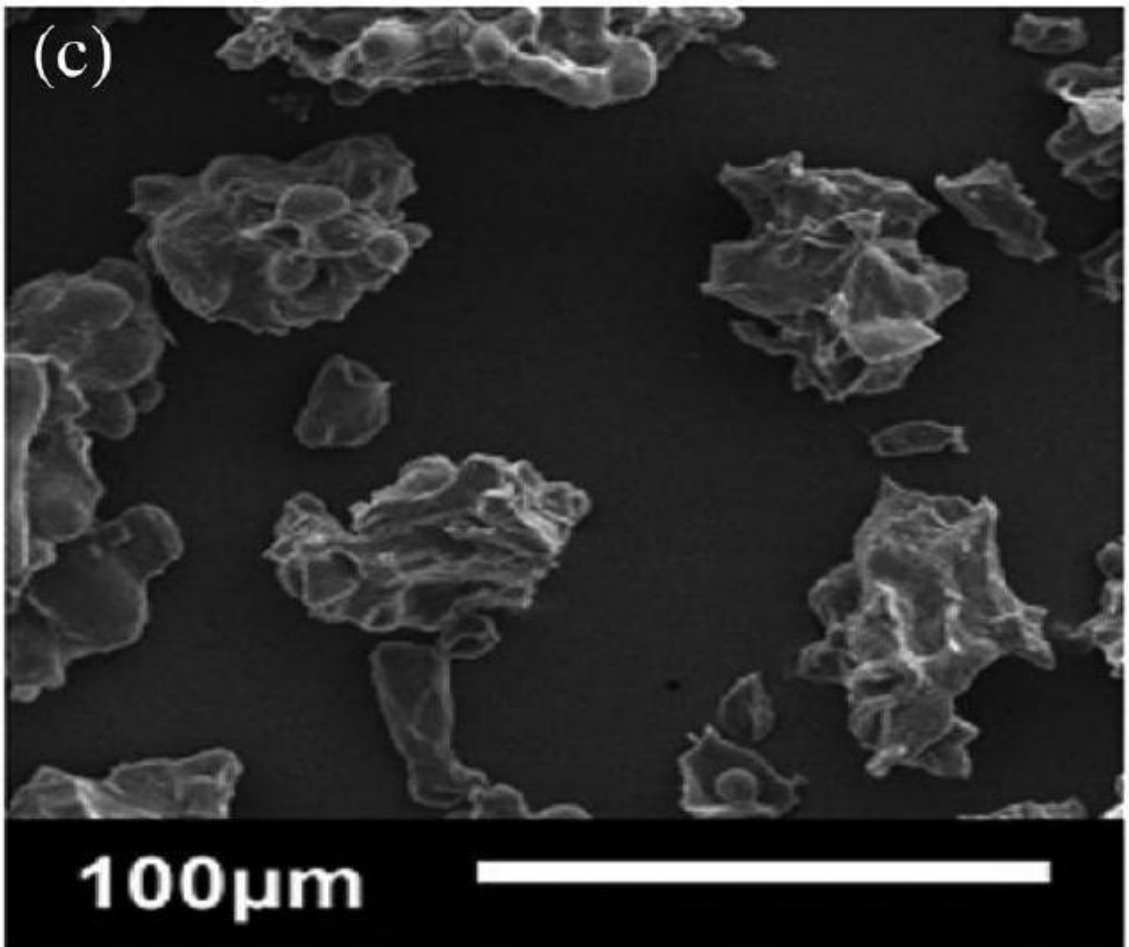
(c)
100μm

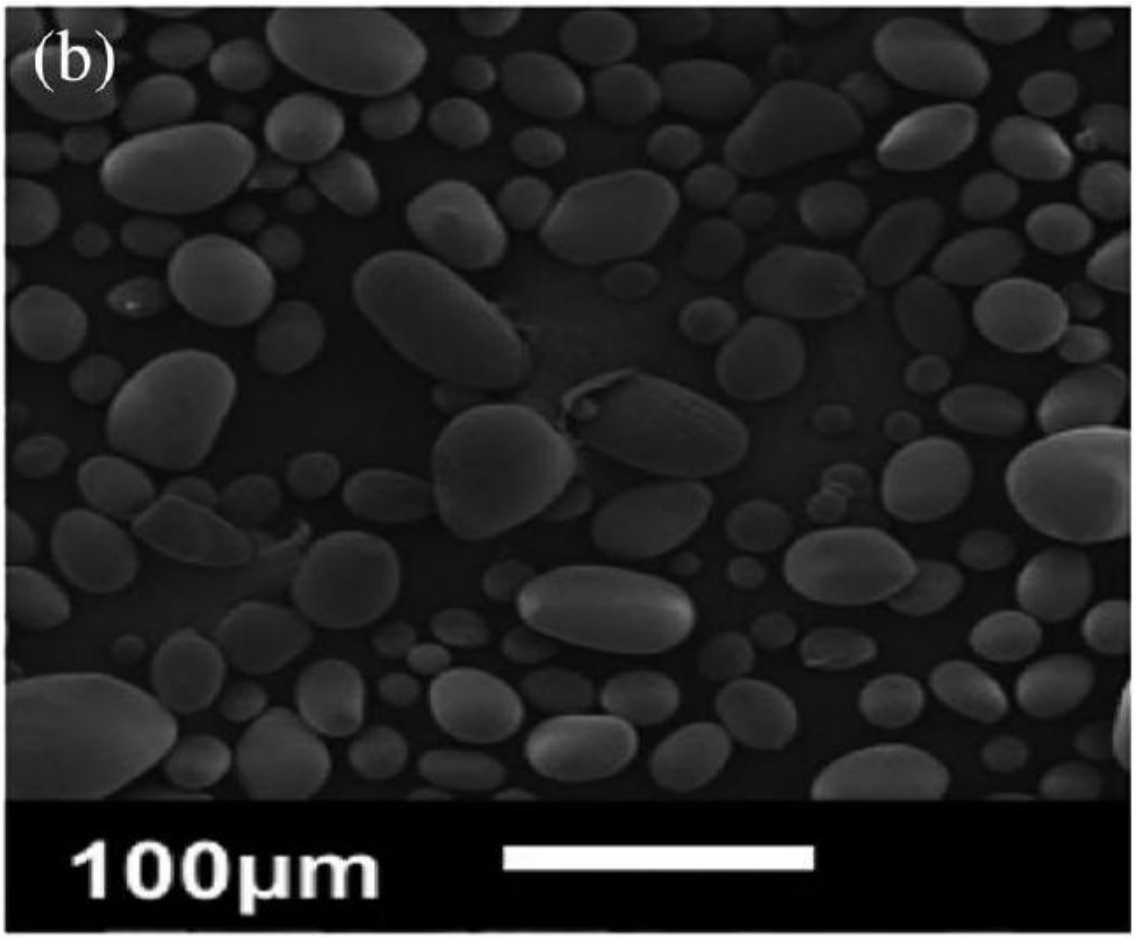
(b)
100µm

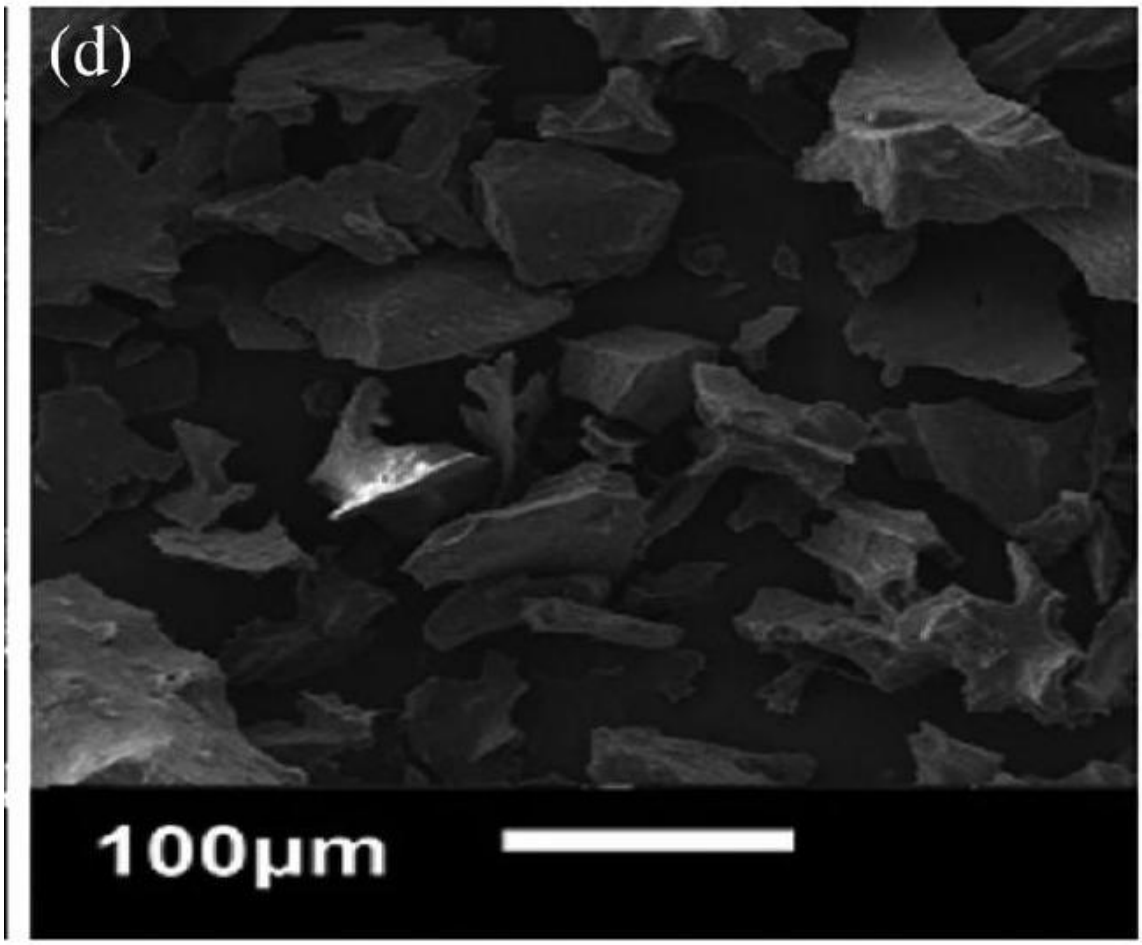
(d)
100µm

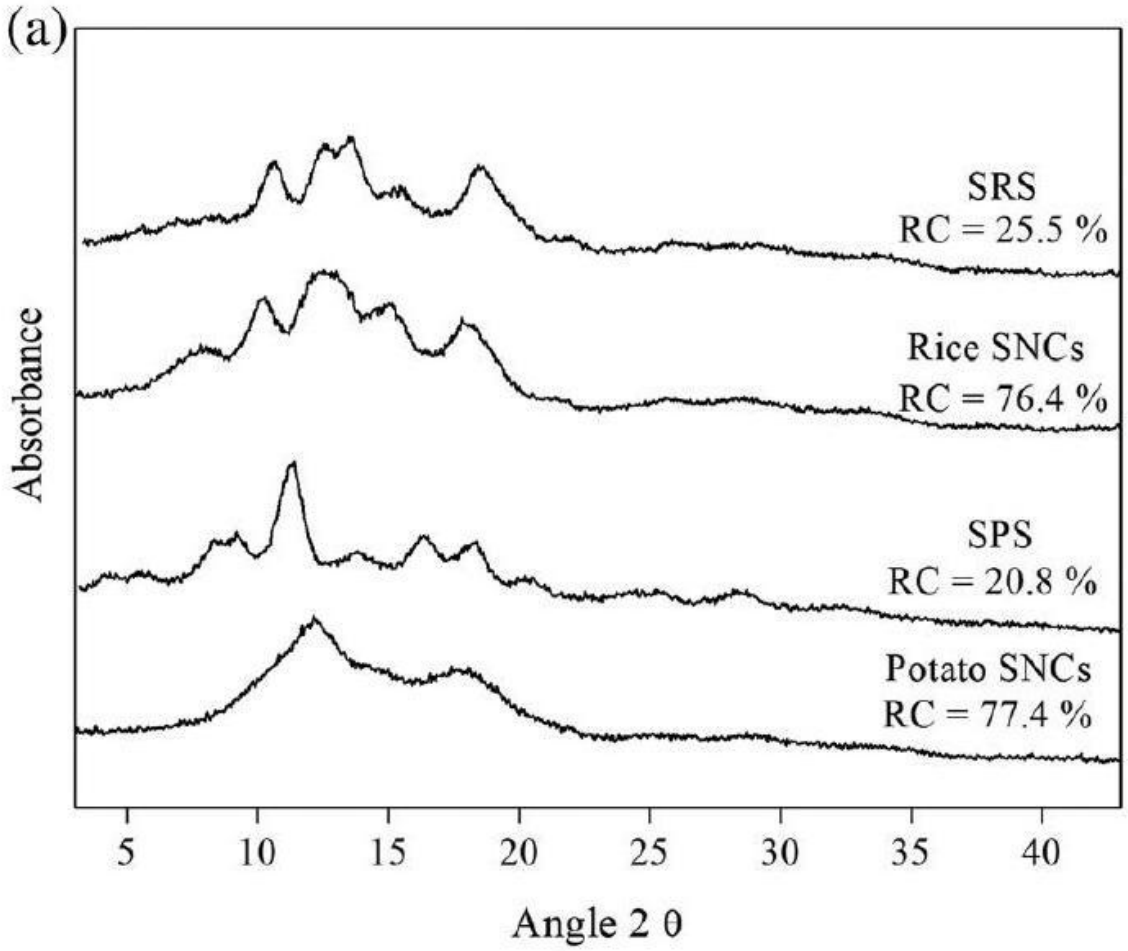
(a)
SRS
RC = 25.5 %
Rice SNCs
RC = 76.4 %
SPS
RC = 20.8 %
Potato SNCs
RC = 77.4 %
Absorbance
5
10
15
20
25
30
35
40
Angle 2 0

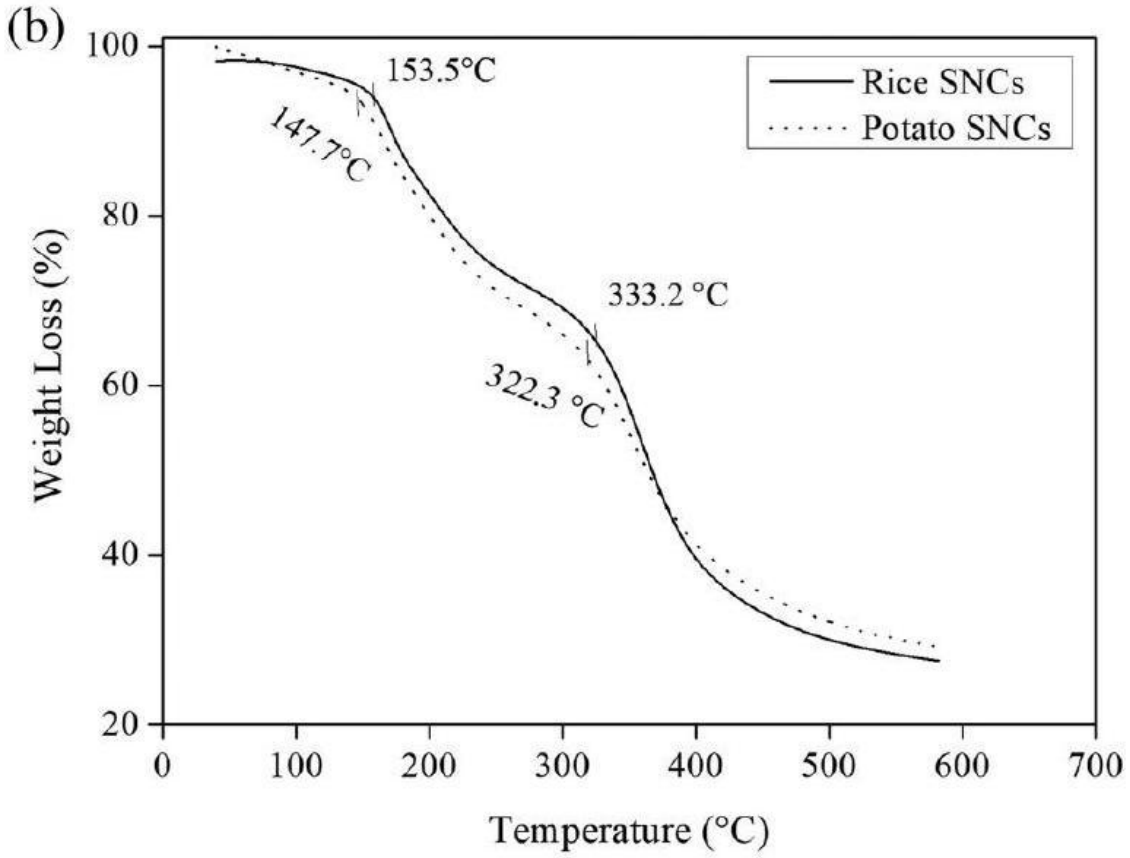

FIGURE 2 (a) Diffractogram and relative crystallinity (RC) of rice starch (SRS), potato starch (SPS), rice starch nanocrystal (rice SNCs) and potato starch nanocrystal (potato SNCs); (b). Thermograms of rice starch nanocrystals (rice SNCs) and potato starch nanocrystals (potato SNCs)

temperature, thus accelerating the weight loss of the material. Thermal characterization of the SNCs was necessary to establish the ideal temperature for the extrusion process. PLA is usually processed at temperatures of 160°C, but this temperature can be modified according to the conditions required for the process. Therefore, from the TGA study it was established that the SNCs could only be applied at maximum temperature of 140°C, thus the material would not degraded during it incorporation in the PLA matrix.

2 | Characterization of PLA and PLA/ SNCs films

1 | Structure characterization

The crystallinity of the PLA and PLA/SNCs films are shown in the XRD diffractograms of Figure 3. All films produced showed a peak in the region between 10 and 25θ characteristic of PLA. Palai et al. [28,29] studied PLA films and observed the same peak in the 2θ region, which

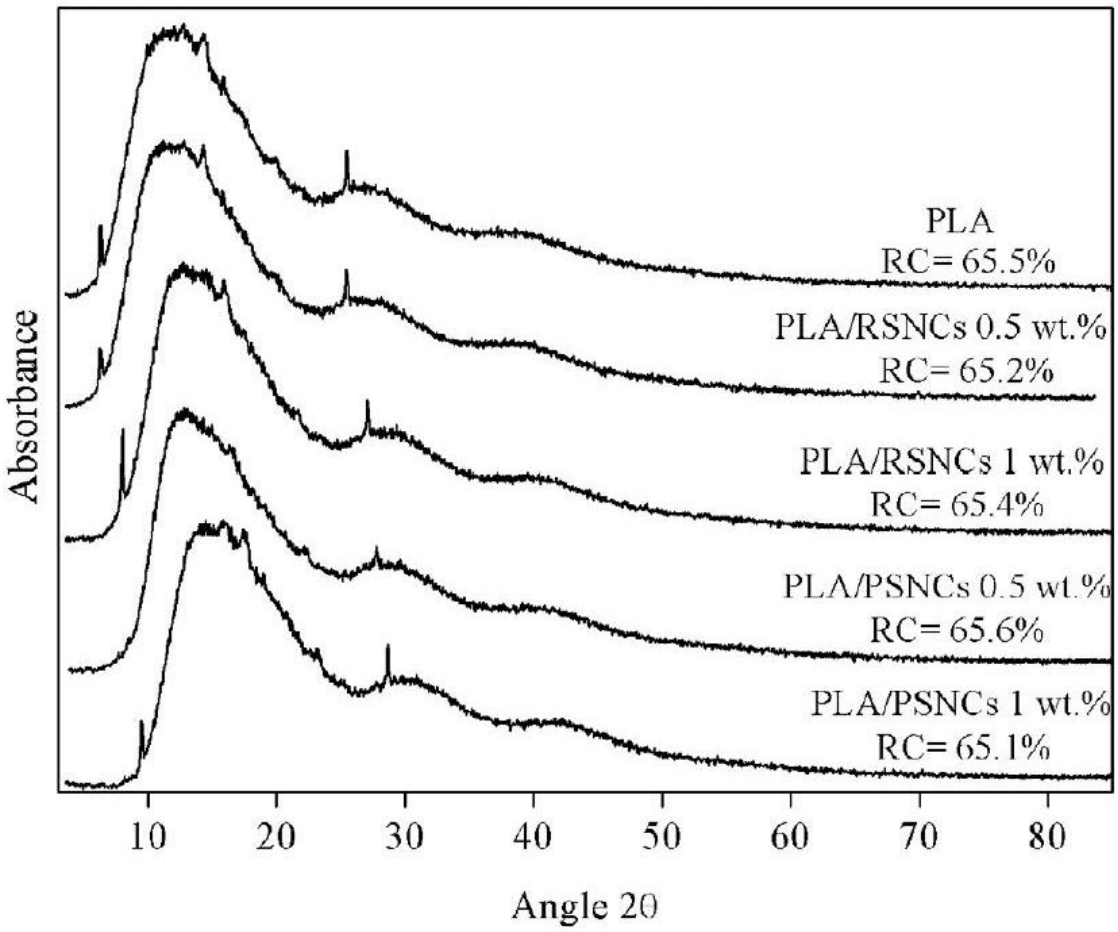

FIGURE 3 Diffractograms and relative crystallinity of PLA and PLA/SNCs nanocomposite films and relative crystallinity characterizes the PLA material. The addition of the SNCs in the PLA matrices did not change the intensity and location of the peaks, consequently, the relative crystallinity that is obtained through the relation between the crystallinity of amorphous and crystalline zones was not affected. The fact that the crystallinity has not been modified confirms the responses of OP and WVP that showed small changes with the addition of the SNCs. According to Sung et al. [6] the crystallinity of the materials is linked to the permeation responses; more crystalline materials are more compact and hinder the percolation of gases.

The micrographs of the PLA and PLA/SNCs nanocomposites (Figure 4) of the films are cohesive and homogeneous. The presence of exposed nanocrystals in the cross-section was not verified, the small white points present in some cuts are due to the continuous matrix fracture caused by liquid nitrogen. The biggest structural difference observed among PLA films and films containing the SNCs was the presence of greater porosity of the films that contain the SNCs. This porosity is believed to be linked to the incorporation of SNCs that may have caused the discontinuity of the film. Wang et al. [30] observed the presence of pores of different sizes throughout the PLA films incorporated with cellulose nanocrystals. This effect was attributed to the release of the water due to the application of evaporation temperatures. Therefore, it is believed that the porosity observed in the PLA/SNCs nanocomposite films may have been caused by the evaporation of water present in the

SNCs (approximately 3%). The porosity observed may be related to the permeability responses, since the films containing the SNCs, in general, showed higher percolation of oxygen gases and water vapor. Sung et al. [6] comments that the process of incorporating nanocrystals in films by the extrusion method is extremely appropriate. The extrusion enhances the homogenization process and forms films with great homogeneity.

2 | Optical properties and hydrophobicity

Figure 5 shows the appearance of the different PLA films produced. The addition of SNCs at a concentration of 0.5% (Figure 5b and Figure 5c) changed the appearance of the films, making them darker in comparison with the control (Figure 5a), but when purchased with films containing SNCS at a concentration of 1% (Figure 5d and Figure 5e) it was observed that increasing the concentration intensified the dark coloration of SNCs.

Table 2 presents the total color difference of the ΔE^* films and the opacity (OP) of the PLA and PLA/SNCs films. The ΔE^* of the films containing the SNCs increased as the concentration of the SNCs was increased. The total color difference is a parameter that assesses global color changes when compared with the equipment standard. The variations presented by $\Delta E*$ indicate that the SNCs were affected by the application of heat during the extrusion process. Therefore, it is believed that during the SNCs incorporation process, the high temperature associated with the presence of carbohydrates of different chain sizes (mono, di, oligosaccharides) may have caused caramelization reactions. [31] The opacity of the films was also influenced by the addition of the SNCs (Table 2). As the concentration of the SNCs increased, the opacity of the films increased significantly compared with the standard. According to Romani et al. [32] the increase in opacity acts as a barrier to the light through the packaging. Packaging intended for food applications, the reduction of light penetration contributes to the reduction of reactions that can deteriorate food, consequently increasing the shelf life of products.

The hydrophobicity of the films was evaluated through the contact angle using water as a solvent (Table 2). The contact angle varies from 0 to 150°, for values below 90° films are considered with hydrophilic nature and for angles above 90° the material has a hydrophobic nature. [33] All the films produced showed hydrophobic nature, as they have an angle greater than 90°. The films (PLA/PSNCs 0.5 and PLA/PSNCs 1wt%) incorporated with SNCs obtained from potato starch demonstrate contact angles statistically equal to each other and statistically different from the control film. The addition of potato SNCs increased the hydrophobic nature of the material, according Slavutsky & Bertuzzi [34] this effect can be attributed to the strong interaction between potato SNCs and the PLA matrix through hydrogen bonding, consequently reducing the availability of interactions with water.

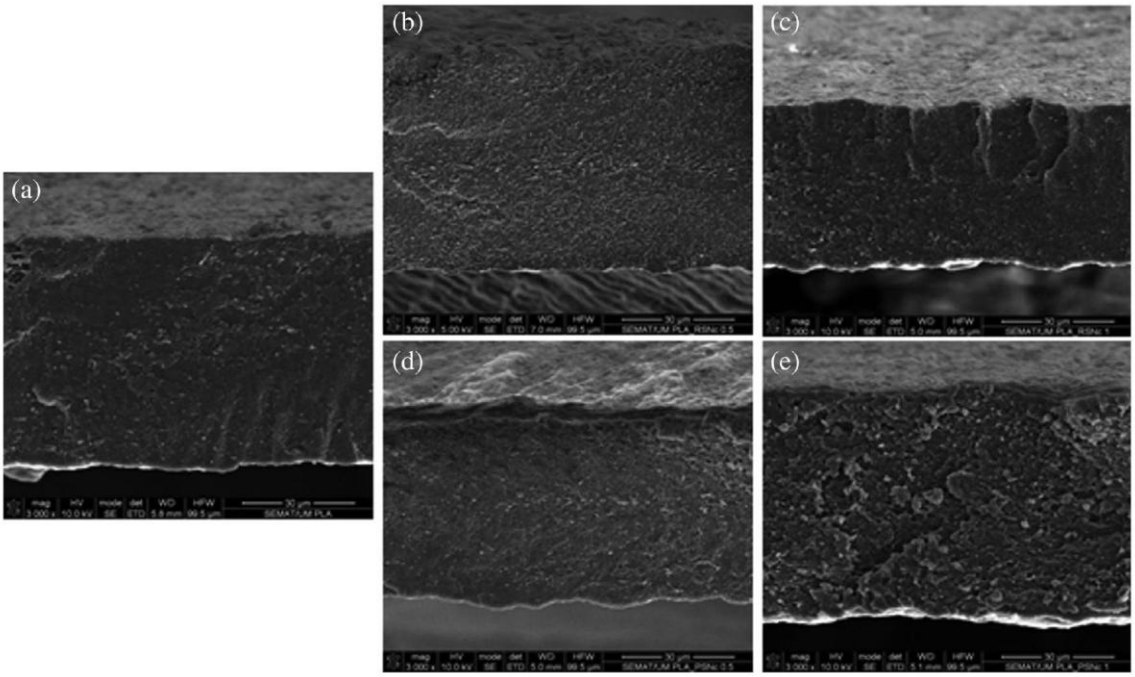

FIGURE 4 Micrograph of the cross-section of the films (a) PLA (control), (b) PLA/RSNCs 0.5wt%, (c) PLA/RSNCs 1wt%, (d) PLA/ PSNCs 0.5wt% (e) PLA/PSNCs 1wt%

FIGURE 5 Image of PLA and PLA/SNCs nanocomposite films. (a) PLA, (b) PLA/RSNCs 0wt%, (c) PLA/PSNCs 0.5wt%, (d) PLA/RSNCs 1wt%, and (e) PLA/PSNCs 1wt%

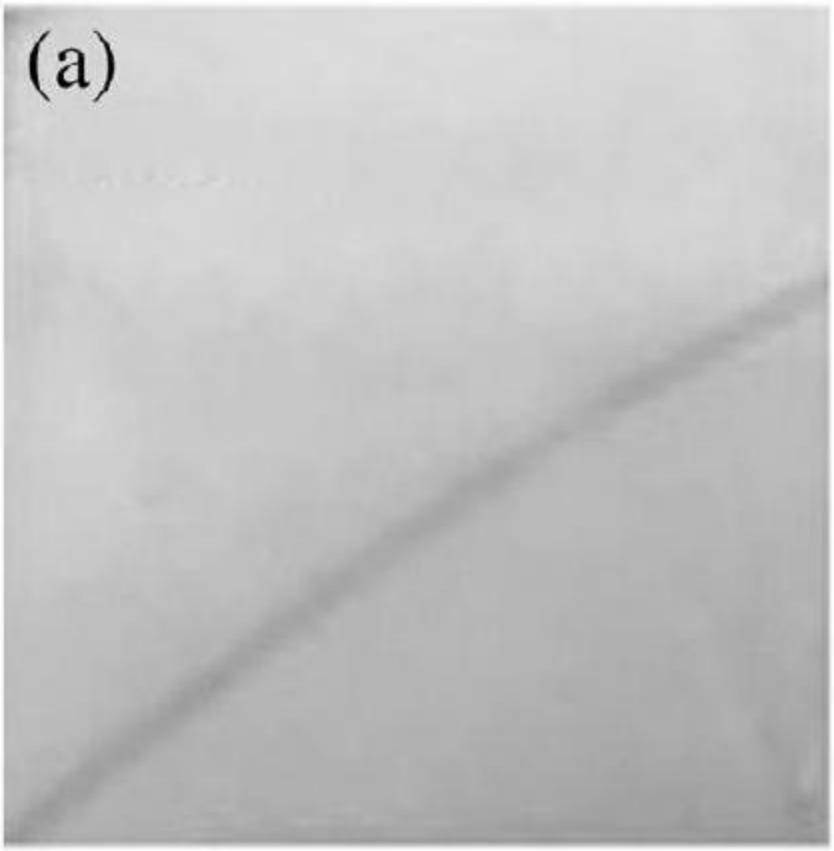
(a)

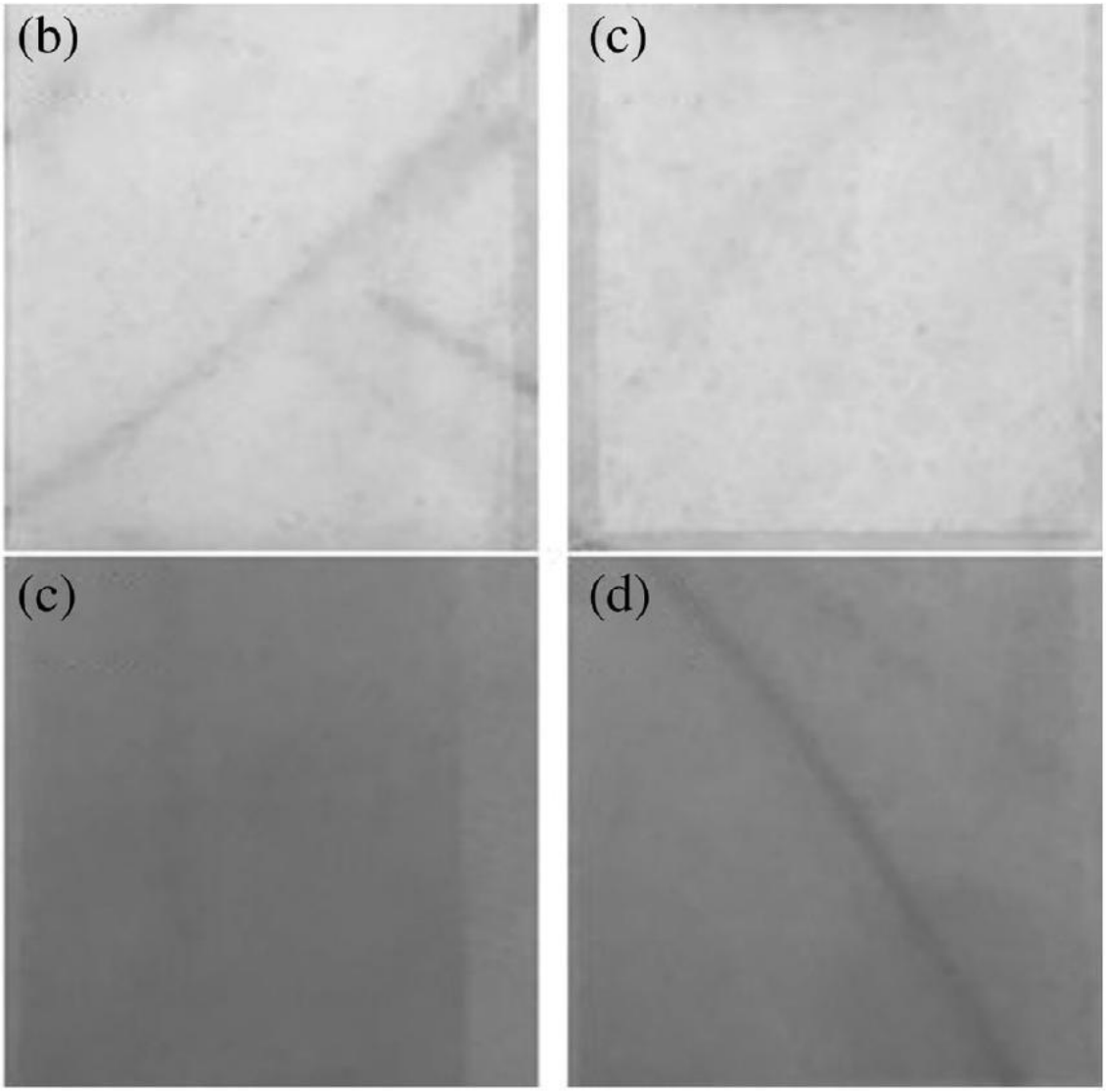

3 | Mechanical properties

Mechanical properties of PLA and PLA nanocomposites films are shown in Table 3. The films were characterized in the longitudinal and transverse directions, since the bi-oriented tubular extruder used to produce the films performs the process of orienting the films in the longitudinal direction. Therefore, bi-orientation changes the properties of the films depending on the direction of the cut. According to Baek et al. [35] variations in the type of

Films	Optical properties		Contact angle (°)
	ΔE*	Opacity (%)	
PLA	$1.07^{e} \pm 0.05$	$29.1^{d} \pm 0.2$	$103.7^{b} \pm 0.3$
PLA/RSNCs 0.5wt%	$2.67^{d} \pm 0.07$	$29.8^{c} \pm 0.2$	$102.6^{c} \pm 0.3$

PLA/RSNCs 1wt%	4.03 ^{b} ± 0.07	31.8 ^{b} +0.6	102.7 ^{c} ± 0.2
PLA/PSNCs 0.5wt%	3.37^{c} ± 0.03	30.2^{c} ± 0.5	108.1 ^{a} ± 0.2
PLA/PSNCs 1wt%	4.36^{a} ± 0.07	35.4 ^{a} ± 0.2	107.9^{a} ± 0.1

Note: Means ± standard deviation. Different letters in the same column indicate significant differences ($p < 0.05$).

TABLE2 Optical properties and contact angle of PLA and PLA/SNCs films

TABLE 3 Mechanical properties of PLA and PLA/SNCs nanocomposite films

Film	Transversal			Longitudinal		
	Elastic modulus (GPa)	Tensile strength (MPa)	Elongation at break (%)	Elastic modulus (GPa)	Tensile strength (MPa)	Elongation at break (%)
PLA	506.8 ^{a} +1.3	18.0^{a} ± 0.5	42.1^{d} ± 3.3	1048 ^{a} + 4.8	36.6 ^{b} ± 0.7	595.8 ^{a} ± 3.7
PLA/RSNCs 0.5wt%	386.1 ^{b} ± 3.1	12.8 ^{b} ± 0.4	88.6^{c} ± 2.1	793.4 ^{b} ± 3.9	24.1 ^{d} ± 0.6	4.9 ^{b} ± 0.3
PLA/RSNCs 1wt%	304.6^{e} ± 1.3	12.2^{b} ± 0.9	88.1 ^{c} ± 1.4	725.8 ^{d} ± 3.7	20.4 ^{e} ± 1.0	5.0^{b} ± 0.3
PLA/PSNCs 0.5wt%	334.6 ^{c} ± 2.9	18.0^{a} ± 0.4	136.6^{a} ± 2.7	584.8 ^{e} ± 2.0	27.6^{c} ± 1.3	5.5 ^{b} ± 0.3
PLA/PSNCs 1wt%	315.4 ^{d} ± 2.2	18.5 ^{a} ± 0.4	129.6 ^{b} ± 3.5	740.2^{c} ± 1.0	38.9^{a} ± 0.7	5.9^{b} ± 0.5

Note: Means ± standard deviation. Different letters in the same column indicate significant differences ($p < 0.05$).
process and the equipment used to obtain the films alter the characteristics of the films produced. Table 3 shows different characteristics of the films in the longitudinal and transversal direction, in addition to the variations caused by the addition of the SNCs. In general, in the longitudinal direction (the stretching direction that the equipment applies to the films) the mechanical properties are superior to those obtained in the transversal direction. According to Rosato et al. [36] this occurs due to the stretching direction applied to the thermoplastic material, which consists of the relation between the axial direction of the material's molecular orientation and the mechanical stress of the polymer, consequently changing the mechanical properties of the material.

EM shows the relation between ratio of stress to elastic strain. The EM was reduced for all films containing SNCs when compared to the control in longitudinal and transversal orientations. The same effect was observed in the study of Baek et al. [35] in some

concentrations of titanium dioxide of the nanocomposite prepared. The reduction in the modulus of elasticity is attributed to the effect caused by the addition of nanomaterials in the PLA matrix, thus increasing the mobility of the polymer chain causing greater brittleness.

The TS of the films in the transversal direction remained statistically equal, around 18 MPa , for the treatments with the addition of 0.5 and 1wt% of PSNCs. For the longitudinal direction, the PLA/PSNCs 1wt% treatment showed an increase in TS from 36.6 (PLA control) to 38.9 MPa . The SNCs obtained from potato starch showed a positive influence, increasing the TS. It is believed that potato SNCs have been homogenized more uniformly in the PLA matrix, as according Wang et al. [30] the proper incorporation of the SNCs in the polymer promotes the formation of hydrogen bonds between the PLA and the hydroxyl groups present in the SNCs. Another important point was the reduction in TS caused by rice SNCs. It is believed that the agglomeration observed in the rice SNCs micrograph may explain this effect. Sung et al. [6] observed similar behavior in their study and attributed this behavior to the agglomeration of nanoparticles, which difficult the adequate incorporation of SNCs into polymers and reduces the capacity of hydrogen bond formation, consequently reducing TS. Baek et al. [35] attributed the reduction of TS in PLA films added with nanocomposites to the formation of agglomerations in the process, the authors complement showing that the addition of nanocomposites can improve the flexibility of PLA films and make them more brittle.

The EB of PLA/SNCs nanocomposites films showed differences for the longitudinal and transversal direction. In the longitudinal direction, the EB was significantly reduced with the addition of the SNCs, while the transversal assessment increased significantly with the addition of the SNCs. Niu et al. [7] observed the reduction of EB with the addition of 10% of nanofibers in the PLA matrix and attributed this behavior to the capacity of the nanomaterial to provide stiffness to the films and consequently reduce the elongation capacity. Sung et al. [6] reported that nanomaterials can have this hardening effect that led to fracture of the material with stress. It is believed that the longitudinal orientation process combined with the addition of the SNCs can cause stiffen to the material and consequently reduce the elongation capacity. However, when it comes to the transversal direction, the SNCs contributed to the increase in the extensibility of the material. The SNCs interacted with the material in order to reduce fracture and to increase the stretching capacity. According Baek et al. [35] the toughness and elongation of the material depends on the process and nanoparticles interaction with the matrix.

Figure 6 shows the DMA evaluation for the PLA control film and the PLA films with rice and potato SNCs 1wt%. The dynamic properties of materials are linked to structural characteristics and the morphology of the polymers and materials formed. [37] Storage modulus (E') was reduced for all treatments in the evaluated temperature range and the addition of the SNCs further reduced the E'. A similar effect was verified by Sanyang et al. [38] that observed that E' decreases as the concentration of nanoparticles increase in the PLA matrix. Related to this, the effect of reducing E' with increasing temperature is attributed by the authors to the amorphous characteristic of the material tan delta is another parameter that can be measured in DMA analyzes, which is associated with glass transition temperature of the material (T_g), the molecular movement of the material that can be defined by the relation between loss modulus and storage modulus (tan delta = E " /E′) [37] The PLA control, PLA RSNCs

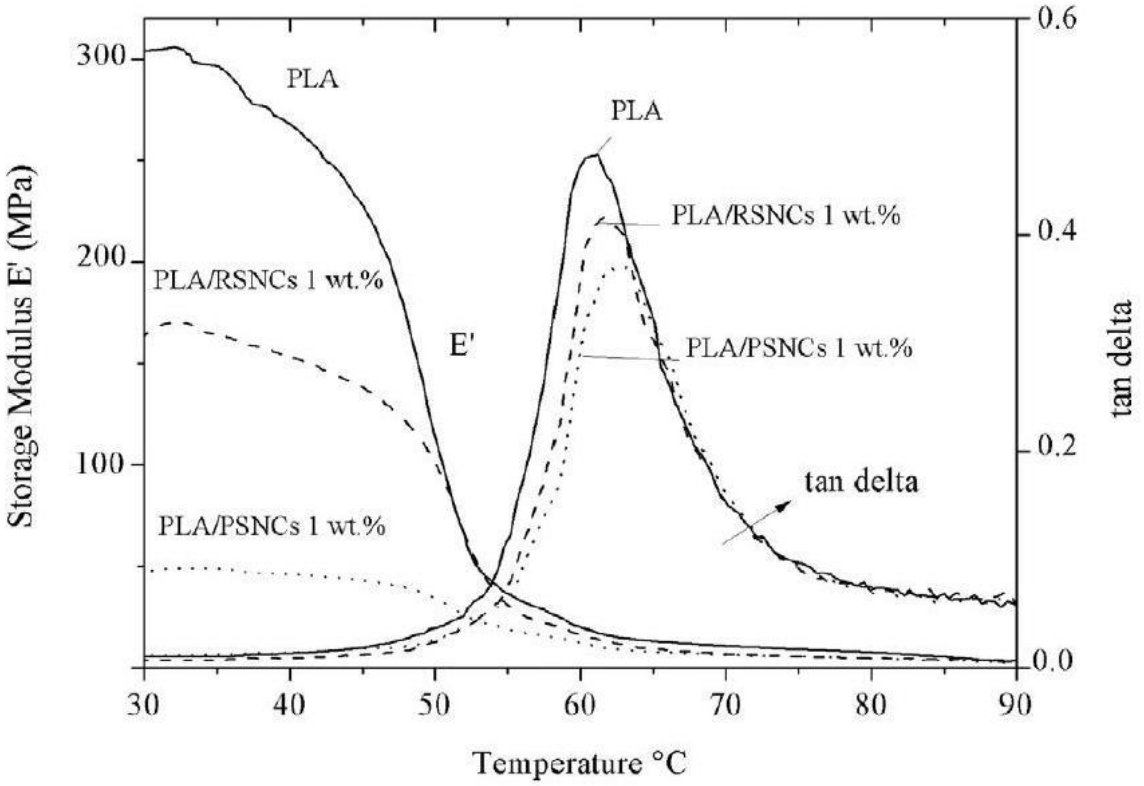

FIGURE 6 Dynamic mechanical analysis spectra of PLA and PLA/SNCs nanocomposite films

1 and, PLA/PSNCs 1wt% films showed a shift of T_g from 58.7,60.5, and 63.1°C, respectively. The glass transition temperature indicates when the polymer chains increase their mobility. Kristo & Biliaderis [39] verified an increase in T_g with the addition of SNCs on a polymeric pullman based and attributed this behavior to the ability of the SNCs to form hydrogen bonds between the SNCs and the amorphous polymer chain, consequently reducing the mobility of the chains and making them more resistant to temperature variations and more brittle, as seen in the tensile tests.

4 | Oxygen permeability and water vapor permeability properties

The OP obtained for the PLA and PLA nanocomposite films is shown in Table 4. PLA films made with the lowest concentrations of the SNCs (0.5wt%) were not evaluated for OP, because the effect caused by the addition of the highest concentration of SNCs was enough. The addition of nanocrystals to the polymeric matrix of the PLA caused a small increase in the oxygen permeability of the films. According Sung et al. [6] variations in oxygen permeability in systems/matrices containing fillers can be altered due to the formation of tortuosities in the system, restricting, or facilitating the percolation of gases. The transmission of gases is also related to factors such as the phenomenon of dissolution, interaction between molecules and gas, influences crystallinity, porosity, and retention capacity. Palai et al. [28] observed a similar effect of OP reduction in PLA films with the addition of starch. This behavior was attributed to changes in the gas transmission system caused by the addition of another constituent (starch) that can alter the molecular

interaction and consequently destabilize the system and contribute to oxygen permeation. Palai et al. [29] comment that PLA has low oxygen permeability, but observed that the addition of Poly (butylene succinate-co-adipate) promotes changes

TABLE 4 Oxygen and water vapor and permeability of PLA and PLA/SNCs nanocomposite films

Films	OP (ml.mm/MPa/ min/cm^2)	WVP (g.mm/ d. m^2. KPa)
PLA	$2.99E-05^{b} \pm 4E-07$	$0.63^{b,c} \pm 0.02$
PLA/RSNCs 0.5wt%	-	$0.66^{b} \pm 0.01$
PLA/RSNCs 1wt%	$3.11E-05^{a} \pm 4E-07$	$0.71^{a} \pm 0.02$
PLA/PSNCs 0.5wt%	-	$0.61^{c} \pm 0.01$
PLA/PSNCs 1wt%	$3.29E-05^{a} \pm 2E-06$	$0.58^{d} \pm 0.02$

Note: Means $\pm$ standard deviation. Different letters in the same column indicate significant differences ($p < 0.05$).
in the material structure and facilitates the permeation of gases, similar behavior was noticed in the present study.

WVP of the PLA and PLA/SNCs nanocomposite films are showed in Table 4. The WVP was significantly changed with the addition of SNCs. The addition of 1wt% rice SNCs to the PLA matrix caused an increase in WVP to 0.71 (g. mm/d · m^2 · KPa), while the addition of 1wt% potato SNCs caused a reduction in WVP to 0.58 (g.mm/d. m^2. KPa). The increase in WPV with the addition of SNCs was reported by Charoenthai et al. [40] that evaluated the addition of cassava SNCs in ethylcellulose and justified this behavior due to the increase in porosity caused by the addition of nanomaterials that can make the matrix discontinuous and increase the water vapor permeation. On the other hand, the reduction in WVP was reported by other authors Kristo & Biliaderis [39] and Li et al.. [15] Both authors attribute this decrease to adequate dispersion of the SNCs maintaining the cohesive matrix, and obstructing the water molecules path. According to Sung et al. [6] WVP can be improved with the addition of nanomaterials dispersed appropriately and with character compatible with the polymer matrix, thus promoting structural reinforcement on a nanometric scale. Another observation was the differences in the behavior of WVP obtained by starches extracted from different sources (rice and potato), it is believed that the differences observed may be linked to the characteristics of the materials such as size, crystallinity, and compatibility among the materials.

5 | Thermal analysis of the films

The thermograms obtained for the PLA and PLA/SNCs nanocomposite films are shown in Figure 7. The thermogram showed that the stage of greatest weight loss of the

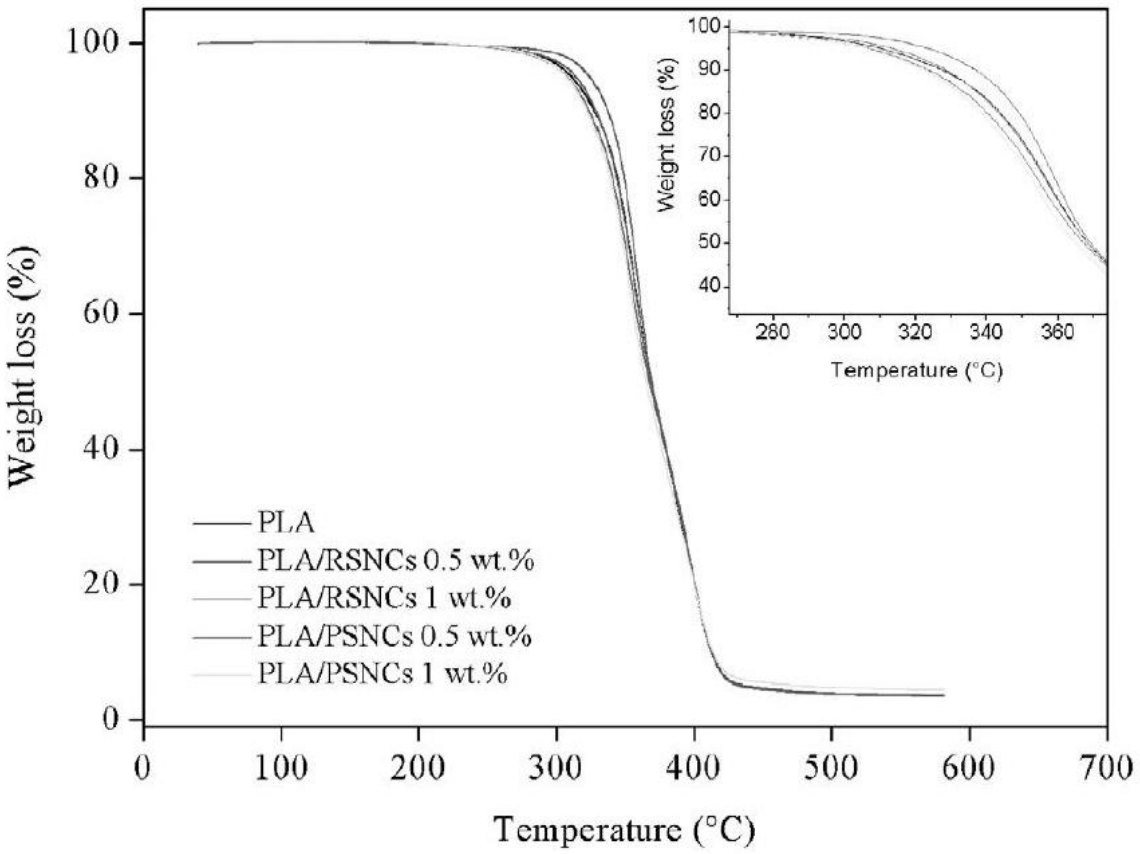

FIGURE 7 TGA thermogram of PLA and PLA/SNCs nanocomposite films films was in the range between 290 and 380°C. Similar degradation temperatures for the PLA were verified by Putri et al. [4] Therefore, the degradation temperature range observed in the thermogram is predominant due to PLA decomposition. The addition of the SNCs to the PLA matrices have a little influence on the degradation temperature, but not enough effect to change the thermal resistance on a large scale. The maximum degradation temperatures observed for the films PLA, PLA/RSNCs 0.5, PLA/RSNCs 1, PLA/PSNCs 0.5, and PLA/PSNCs 1 wt % were 357.7, 353.9, 356.6, 359.2, and 353.8°C, respectively. Orsuwan et al. [41] evaluated the incorporation of silver nanoparticles in a polysaccharide matrix and found no effect on the increase in the material's degradation temperature, similar to the effect observed in this study. According to the thermogram of the SNCs (Figure 2b) the temperature of greatest weight loss is around 330°C, however, the maximum degradation temperature of the SNCs is lower than PLA, the addition of the SNCs did not influence the global degradation temperature indicating the homogeneity of PLA/SNCs nanocomposites films.

4 | CONCLUSION

The application of both SNCs promoted changes in the properties of the produced PLA films. However, the SNCs produced from potato starch caused major changes in the films. The tensile strength in the longitudinal section increased to 38.9 MPa with the addition of PSNCs 1wt% while the control film showed 36.6 MPa . Along with this, in the evaluation of the mechanical properties, in the transversal direction of the films, the films produced with PSNCs 0.5wt% showed an elongation of 136.6%, corresponding to 3 times more than

the elongation of the control film (42.2%). Oxygen permeability increased with the addition of the SNCs, however, the WVP was reduced with the addition of PSNCs 1wt% when compared with the control film. Regarding the structure of the films, the relative crystallinity was not affected with the addition of the SNCs, however, the cross-sectional micrographs showed structural changes, the addition of the SNCs increases the porosity of the films. Another important point was the increase in the glass transition temperature with the addition of PSNCs 1wt%, which increased from 58.7 (control) to 63.1°C. Therefore, the addition of PSNCs at a concentration of 1% promoted improvements in PLA films, making them more resistant and expanding commercial applicability.

ACKNOWLEDGEMENTS

This research was developed within the scope of the Capes-PrInt Program (Process # 88887.310848/2018-00). Authors thank the National Council for Scientific and Technological Development (CNPq) of Brazil and the

Brazilian Coordination for the Improvement of Higher Education Personnel (CAPES) [Finance Code 001].

REFERENCES

[1] A. Etxabide, J. Uranga, P. Guerrero, K. Caba, Food Hydrocolloids 2016, 1-7, 192.
[2] M. Murariu, P. Dubois, Adv. Drug Delivery Rev. 2016, 107, 17.
[3] T. Hussain, M. Tausif, M. Ashraf, J. Cleaner Prod. 2015, 108, 476.
[4] N. Putri, S. Hajar, R. Kadir, R. A. Talib, Food Packag. Shelf Life J. 2020, 23, 450.
[5] M. A. Elsawy, K. Kim, J. Park, A. Deep, Renewable Sustainable Energy Rev. 2017, 79, 1346.
[6] S. H. Sung, Y. Chang, J. Han, Carbohydr. Polym. 2017, 169, 495.
[7] X. Niu, Y. Liu, Y. Song, J. Han, H. Pan, Carbohydr. Polym. 2018, 183, 102.
[8] I. Joye, Encyclopedia of Food and Health. (Eds: P. Varelis, L. Melton, F. Shahidi), Elsevier Inc., Netherlands 2019, p. 256.
[9] S. Damodaran, K. L. Parkin, O. R. Fennema, Química de Alimentos de Fennema (4°). Artmed. 2010
[10] Concha, B. B. Sanchez, E. Agama-Acevedo, M. C. NuñezSantiago, L. A. Bello-Perez, H. S. Garcia, J. Alvarez-Ramirez, J. Cereal Sci. 2018, 79, 193.
[11] Y. Hao, Y. Chen, Q. Li, Q. Gao, Carbohydr. Polym. 2017, 184, 171.
[12] M. Eliacin, F. Scaraglino, Carbohydr. Polym. 2018, 180, 122.
[13] A. Dufresne, Curr. Opin. Colloid Interface Sci. 2014, 19, 397.
[14] Q. Sun, Starch in Food: Structure, Function and Applications, 2nd ed. (Eds: M. Sjöö, L. Nilsson), Woodhead Publishing, Cambridge 2018, p. 691.
[15] X. Li, C. Qiu, N. Ji, C. Sun, L. Xiong, Q. Sun, Carbohydr. Polym. 2015, 121, 155.
[16] J. Mao, Y. Tang, R. Zhao, Y. Zhou, Z. Wang, J. Polym. Environ. 2019, 27, 728.
[17] K. Jin, Y. Tang, X. Zhu, Y. Zhou, Int. J. Biol. Macromol. 2020, 162, 1109.
[18] L. E. Velásquez-Castillo, M. A. Leite, S. Ditchfield, P. J. A. Sobral, I. C. F. Moraes, Int. J. Biol. Macromol. 2020, 143, 93.
[19] J. Zhou, J. Tong, X. Su, L. Ren, Int. J. Biol. Macromol. 2016, 91, 186.
[20] P. J. A. Sobral, F. C. Menegalli, M. D. Hubinger, M. A. Roques, Food Hydrocolloids 2001, 15, 423.
[21] ASTM. (2002). Standard test methods for tensile properties of thin plastic sheeting,

D882-02. American Society for Testing and Material.
[22] ASTM. (2000). Standard test methods for water vapor transmission of material E96-00. American Society for Testing and Material.
[23] P. C. Martins, J. M. Latorres, V. G. Martins, LWT-Food Sci. Technol. 2022, 156, 41.
[24] A. Mukurumbira, M. Mariano, A. Dufresne, J. J. Mellem, E. O. Amonsou, Int. J. Biol. Macromol. 2017, 102, 241.
[25] L. Ren, Z. Dong, M. Jiang, J. Tong, J. Zhou, Ind. Crops Prod. 2014, 59, 115.
[26] N. Hari, S. Francis, A. G. R. Nair, A. J. Nair, Food Packag. Shelf Life 2018, 16, 69.
[27] D. Lecorre, J. Bras, A. Dufresne, Carbohydr. Polym. 2012, 87, 658.
[28] B. Palai, M. Biswal, S. Mohanty, S. K. Nayak, Ind. Crops Prod. 2019, 141, 748.
[29] B. Palai, S. Mohanty, S. K. Nayak, Polym. Test. 2020, 83, 106.
[30] X. Wang, Y. Tang, X. Zhu, Y. Zhou, X. Hong, Y. Tang, X. Zhu, Y. Zhou, X. Hong, Int. J. Biol. Macromol. 2020, 146, 1069.
[31] V. Goudarzi, I. Shahabi-Ghahfarrokhi, Int. J. Biol. Macromol. 2018, 116, 1082.
[32] V. P. Romani, C. Prentice-Hernández, V. G. Martins, Ind. Crops Prod. 2017, 97, 268.
[33] F. M. Michael, M. Khalid, R. Walvekar, H. Siddiqui, A. B. Balaji, Biodegradable and Biocompatible Polymer Composites. (Eds: N. Shimpi), Woodhead Publishing, Cambridge 2018, p. 33.
[34] A. M. Slavutsky, M. A. Bertuzzi, Carbohydr. Polym. 2014, 110, 53.
[35] N. Baek, Y. T. Kim, J. E. Marcy, S. E. Duncan, S. F. O. Keefe, Food Packag. Shelf Life 2018, 17, 30.
[36] D. V. Rosato, D. V. Rosato, M. V. Rosato, in Plastic Product Material and Process Selection Handbook, Vol. 5 (Eds: D. V. Rosato, D. V. Rosato, M. V. Rosato), Elsevier, Netherlands 2004, p. 227.
[37] O. Lopez, M. A. Garcia, M. A. Villar, A. Gentili, M. S. Rodriguez, L. Albertengo, LWT-Food Sci. Technol. 2014, 57, 106.
[38] M. L. Sanyang, S. M. Sapuan, M. Jawaid, M. R. Ishak, J. Sahari, Carbohydr. Polym. 2016, 146, 36.
[39] E. Kristo, C. G. Biliaderis, Carbohydr. Polym. 2007, 68, 146.
[40] N. Charoenthai, A. Wickramanayaka, S. Sungthongjeen, S. Puttipipatkhachorn, J. Drug Delivery Sci. Technol. 2018, 47, 283.
[41] A. Orsuwan, S. Shankar, L. F. Wang, R. Sothornvit, J. W. Rhim, Food Hydrocolloids 2016, 60, 476.